Supporting Information

Efficient Oxidation of Methyl Glycolate to Methyl Glyoxylate Using a Fusion Enzyme of Glycolate Oxidase, Catalase and Hemoglobin

Xiangxian Ying [1,*], Can Wang [1], Shuai Shao [1], Qizhou Wang [1], Xueting Zhou [1], Yanbing Bai [2], Liang Chen [2], Chenze Lu [3], Man Zhao [1] and Zhao Wang [1]

[1] Key Laboratory of Bioorganic Synthesis of Zhejiang Province, College of Biotechnology and Bioengineering, Zhejiang University of Technology, Hangzhou 310014, China; m17816035735@163.com (C.W.); ss1964241742@163.com (S.S.); W2936716405@163.com (Q.W.); sadie598851321@163.com (X.Z.); mzhao@zjut.edu.cn (M.Z.); hzwangzhao@zjut.edu.cn (Z.W.)

[2] Hangzhou Xinfu Science & Technology Co., Ltd., Hangzhou 311301, China; byb@xinfupharm.com (Y.B); chenliang201006@163.com (L.C.)

[3] College of Life Sciences, China Jiliang University, Hangzhou 310018, China; chenzelu@cjlu.edu.cn (C.L.)

* Correspondence: yingxx@zjut.edu.cn; Tel.: +86-571-88320781

Contents

Supplementary tables

Table S1. The primers for the construction of the fusion genes encoding *Vs*HGB-linker-*So*GOX-linker-*Hp*CAT [a]

Primer	Sequence
pET28a-*Vs*HGB-F	5′-ATGGGTCGCGGATCCGAATTCATGCTGGACCAGCAGACCAT-3′
pET28a-*Hp*CAT-R	5′-CTCGAGTGCGGCCGCAAGCTTAAGAAAACTTGGTAAACCTTTAGCA-3′
*Vs*HGB-GSG-R	5′-GTGATTTCCATTCCACTTCCTTCAACTGCCTGAGCGTACAGA-3′
*Vs*HGB-GGGGS-R	5′-GTGATTTCCATACTTCCTCCTCCTCCTTCAACTGCCTGAGCGTACAGA-3′
GSG-*So*GOX-F	5′-CAGGCAGTTGAAGGAAGTGGAATGGAAATCACCAACGTTAACG-3′
GGGGS-*So*GOX-F	5′-CAGGCAGTTGAAGGAGGAGGAGGAAGTATGGAAATCACCAACGTTAACG-3′
*So*GOX-GSG-R	5′-GGTCTTGACTCATTCCACTTCCCAGGCGAGCAACAGCACG-3′
*So*GOX-GGGGS-R	5′-GGTCTTGACTCATACTTCCTCCTCCTCCCAGGCGAGCAACAGCACG-3′
GSG-*Hp*CAT-F	5′-TGTTGCTCGCCTGGGAAGTGGAATGAGTCAAGACCCTAAAAAATGTC-3′
GGGGS-*Hp*CAT-F	5′-TTGCTCGCCTGGGAGGAGGAGGAAGTATGAGTCAAGACCCTAAAAAATGTC-3′
pET28a-F	5′-AAGCTTGCGGCCGCACTCGAG-3′
pET28a-R	5′-GAATTCGGATCCGCGACCCAT-3′

[a] The linker is GSG or GGGGS.

Table S2. The primers for the construction of the fusion genes encoding *Hp*CAT-linker-*So*GOX-linker-*Vs*HGB [a]

Primer	Sequence
pET28a-*Hp*CAT-F	5′-ATGGGTCGCGGATCCGAATTCATGAGTCAAGACCCTAAAAAATGTC-3′
pET28a-*Vs*HGB-R	5′-CTCGAGTGCGGCCGCAAGCTTTTCAACTGCCTGAGCGTACAG-3′
*Hp*CAT-GSG-R	5′-CGTTGGTGATTTCCATTCCACTTCCAAGAAAACTTGGTAAACCTTTAGCA-3′
*Hp*CAT-GGGGS-R	5′-GTGATTTCCATACTTCCTCCTCCTCCAAGAAAACTTGGTAAACCTTTAGCA-3′
GSG-*So*GOX-F	5′-CCAAGTTTTCTTGGAAGTGGAATGGAAATCACCAACGTTAACG-3′
GGGGS-*So*GOX-F	5′-CCAAGTTTTCTTGGAGGAGGAGGAAGTATGGAAATCACCAACGTTAACG-3′
*So*GOX-GSG-R	5′-TCCAGCATTCCACTTCCCAGGCGAGCAACAGCACG-3′
*So*GOX-GGGGS-R	5′-TCCAGCATACTTCCTCCTCCTCCCAGGCGAGCAACAGCACG-3′
GSG-*Vs*HGB-F	5′-CTGTTGCTCGCCTGGGAAGTGGAATGCTGGACCAGCAGACCAT-3′
GGGGS-*Vs*HGB-F	5′-TTGCTCGCCTGGGAGGAGGAGGAAGTATGCTGGACCAGCAGACCAT-3′
pET28a-F	5′-AAGCTTGCGGCCGCACTCGAG-3′
pET28a-R	5′-GAATTCGGATCCGCGACCCAT-3′

[a] The linker is GSG or GGGGS.

Table S3. The primers for directed evolution of *So*GOX

Primer	Sequence
*So*GOX-F	5′-ATGGGTCGCGGATCCGAATTCATGGAAATCACCAACGTTAACG-3′
*So*GOX-R	5′-CTCGAGTGCGGCCGCAAGCTTCAGGCGAGCAACAGCACG-3′
pET28a-F	5′-AAGCTTGCGGCCGCACTCGAG-3′
pET28a-R	5′-GAATTCGGATCCGCGACCCAT-3′

Table S4. The primers for site-saturation mutagenesis at sites M267 and S362 of *So*GOX

Primer [a]	Sequence [b]
M267X-F	5′-TCCGGCCACAATTNNNGCACTGGAGGAAGT-3′
M267X-R	5′-ACTTCCTCCAGTGCNNNAATTGTGGCCGGA-3′
S362X-F	5′-ATTGGGATGGACCGNNNTCACGTGCTGTTGC-3′
S362X-R	5′-GCAACAGCACGTGANNNCGGTCCATCCCAAT-3′

[a] X in the name of the primers represented any of 20 standard amino acids. [b] N in the primer sequences represented A, T, C or G and the code to introduce the substitution was underlined.

Table S5. The primers for the construction of the recombinant plasmid pET28a-*Vs*HGB-GSG-*So*GOX^{mut}-GGGGS-*Hp*CAT

Primer	Sequence [a]
M267T-F	5′-ACAATTACTGCACTGGAGGAACTTGTTAAAGC-3′
M267T-R	5′-TCCAGTGCAGTAATTGTGGCCGGAACATAATC-3′
S362G-F	5′-TGGACCGGGTTCACGTGCTGTTGCTCGCCTG-3′
S362G-R	5′-CACGTGAACCCGGTCCATCCCAATCTGCTGC-3′

[a] The code to introduce the substitution was underlined.

Supplementary figures

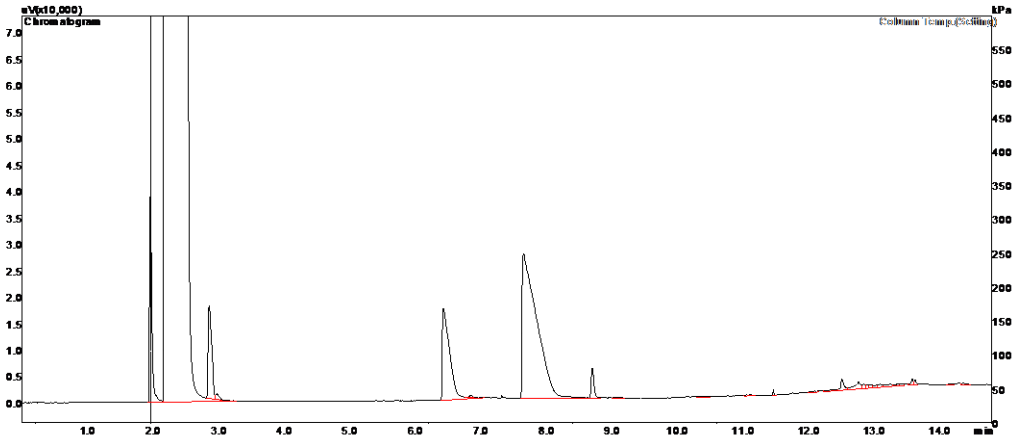

(a)

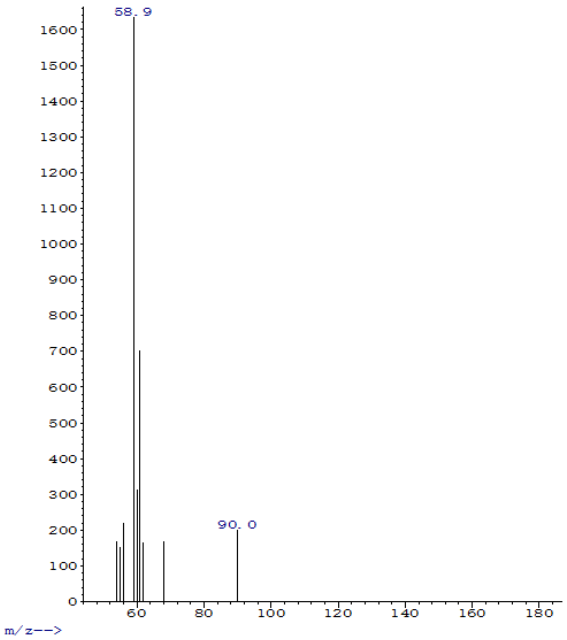

(b)

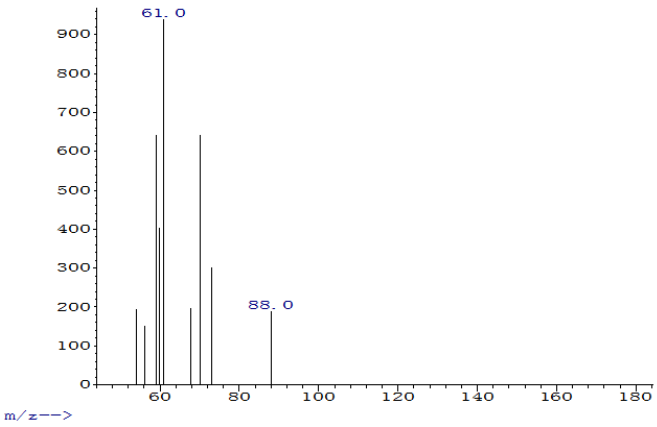

(c)

Figure S1. The GC and GC-MS analyses of methyl glycolate and methyl glyoxylate. (a) GC chromatogram. (b) GC-MS chromatogram for methyl glycolate (MW 90). (c) GC-MS chromatogram for methyl glyoxylate (MW 88).

The GC analyses were conducted using the GC (Agilent 6890N) equipped with an FID detector and chiral capillary BGB-174 column (BGB Analytik, Switzerland, 30 m×250 μm×0.25 μm). The flow rate and split ratio of N_2 as the carrier gas were set as 4 mL/min and 1: 10, respectively. The temperatures for both injector and detector were set as 250 °C. The column temperature program was listed as follows: initial temperature of 70 °C, 5 °C/min ramp to 100 °C for 2 min, and 25 °C/min ramp to 220 °C for 2 min. The injection volume was 1 μL. The retention times for methyl glycolate and methyl glyoxylate were 7.65 and 6.42 min, respectively. The GC-MS analysis (Agilent 7890A/5975C, Agilent Technologies, USA) comprised the following parameters: auxiliary heating zone temperature, 250 °C; MS quadrupole temperature,150 °C; ion source temperature, 230 °C; scan quality range, 30–500 amu; emission current, 200 μA; and electron energy, 70 eV.

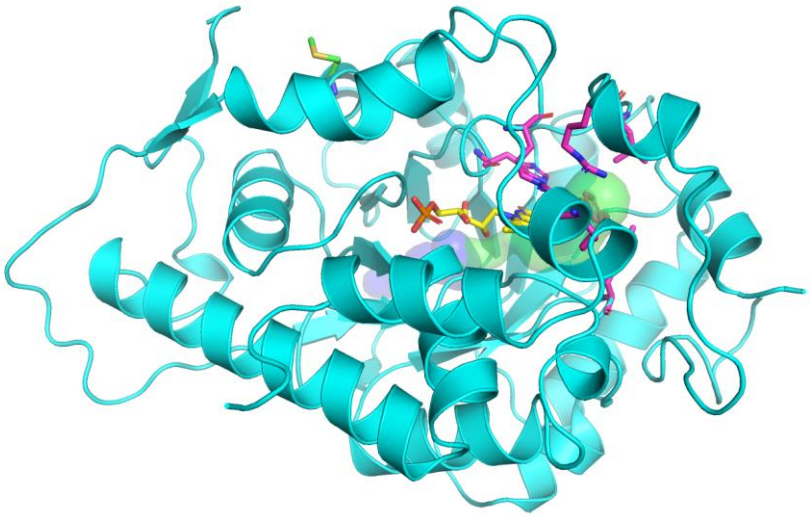

（a）

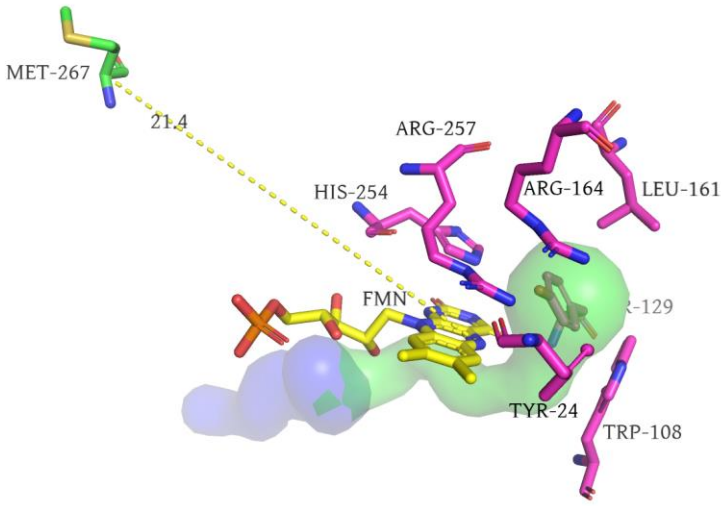

(b)

Figure S2. The structure of *So*GOX and its mutation site. (a) The structure of the *So*GOX monomer (PDB code: 1GOX) and (b) the structure of the active site. Green-colored residues are shaped to allow substrate entrance. The yellow dotted line indicates the distance between Cα of the mutation site and FMN N5. The image was prepared using The PyMOL Molecular Graphics System, and the tunnel calculation was performed by CAVER 3.0.1.

Using the crystal structure of *So*GOX (PDB number: 1GOX), molecular docking simulation was performed using AutoDock Vina under the default docking parameters [1]. Point charges were initially assigned according to the AMBER03 force field and then damped to mimic the less polar Gasteiger charges [2]. Methyl glycolate acted as a ligand to molecular docking with *So*GOX, and the calculation of geometric parameters and ligand structure was performed by

ChemBioDraw 12.0 (CambridgeSoft, Cambridge, MA, USA). To make the results more accurate, 20 consecutive runs were performed and the highest ranked score from each run was used to calculate the average score of each flexible ligand configuration. The docking result with the minimal binding energy value was selected from 100 predictions. The visualization of the resulting substrate–enzyme complexes was processed using the PyMol software [3].

References

1. Trott, O.; Olson, A. J. AutoDock Vina: improving the speed and accuracy of docking with a new scoring function, efficient optimization, and multithreading. J. Comput. Chem. 2010, 31, 455–461.
2. Duan, Y.; Wu, C.; Chowdhury, S.; Lee, M.C.; Xiong, G.M.; Zhang, W.; Yang, R.; Cieplak, P.; Luo, R.; Lee, T.; Caldwell, J.; Wang, J.; Kollman, P. A point-charge force field for molecular mechanics simulations of proteins based on condensed-phase quantum mechanical calculations. J. Comput. Chem. 2003, 24, 1999–2012.
3. Seeliger, D.; de Groot, B.L. Ligand docking and binding site analysis with PyMOL and Autodock/Vina. J. Comput. Aided Mol. Des. 2010, 24, 417-422.

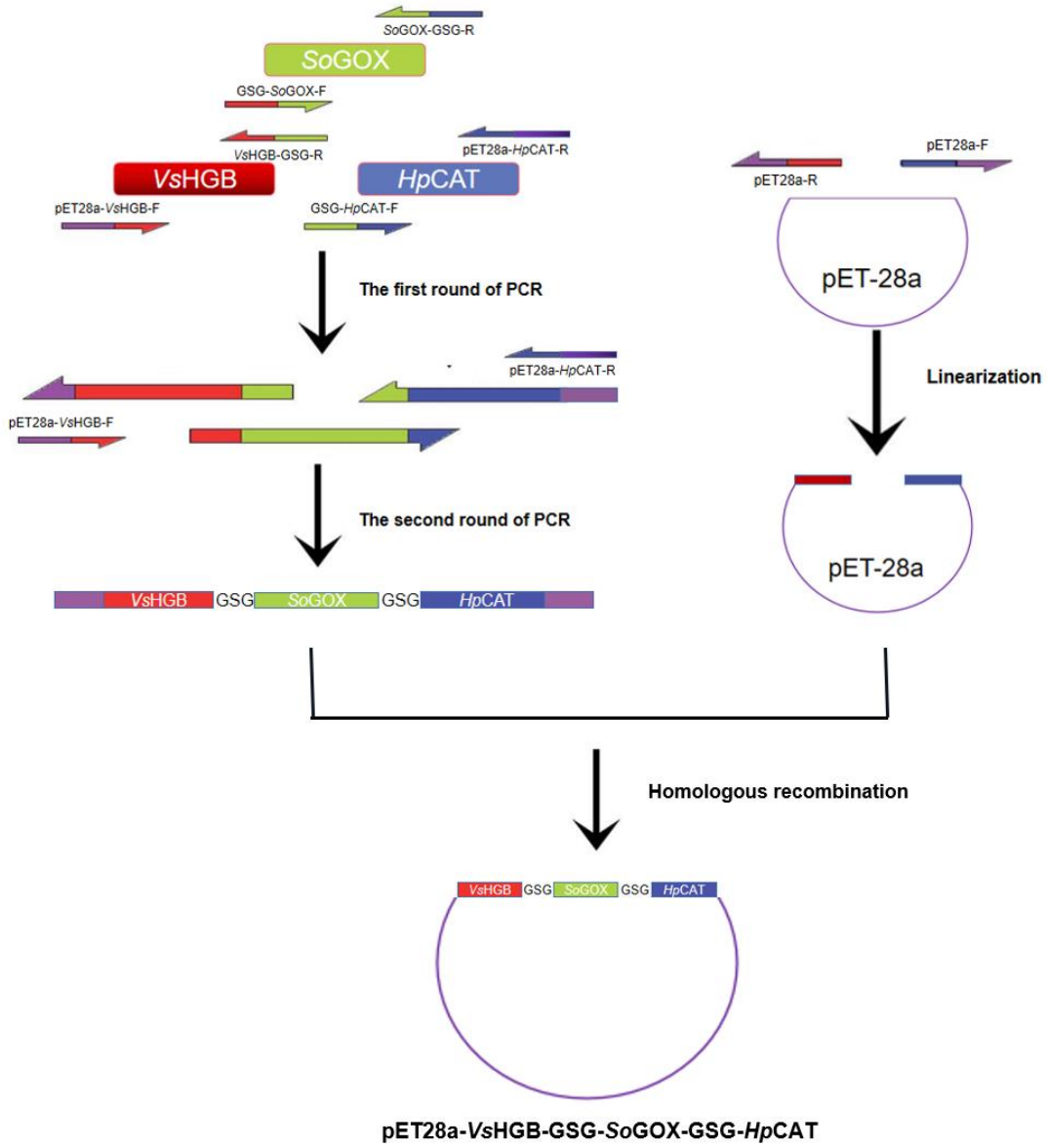

Figure S3. The procedure for the construction of the recombinant plasmid pET28a-*Vs*HGB-GSG-*So*GOX-GSG-*Hp*CAT.

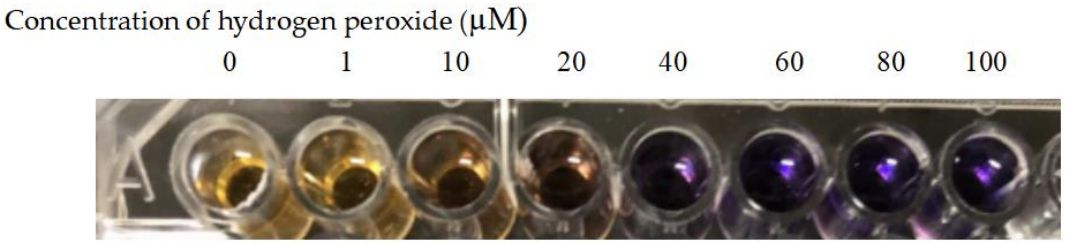

Figure S4. The colorimetric assay for the determination of H_2O_2. In the colorimetric assay, H_2O_2 oxidized Fe^{2+} to Fe^{3+}, which then combined with dye molecules to produce purple Fe^{3+}-dye complexes. The concentrations of H_2O_2 were measured by detecting the absorbance at 595 nm.

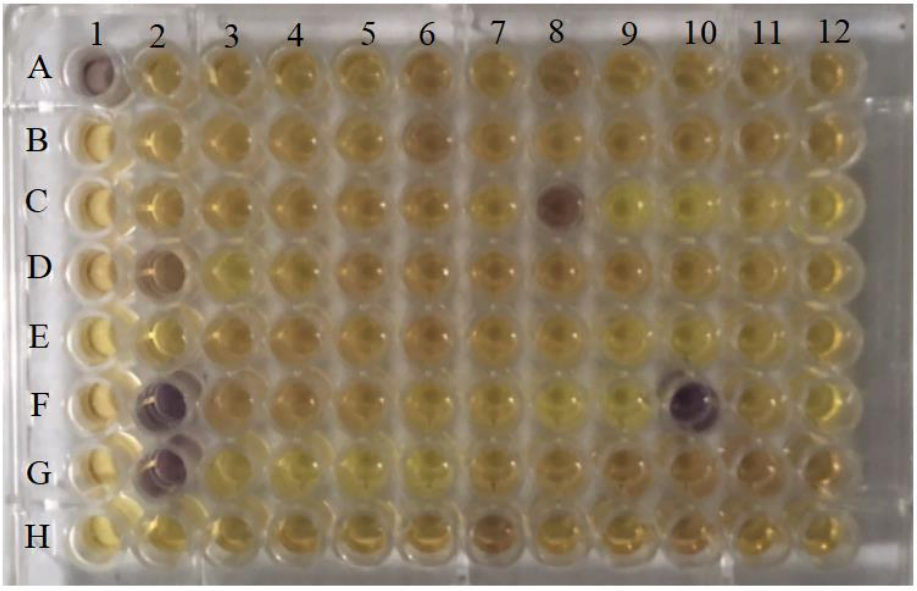

Figure S5. Primary screening of the evolved mutants based on the detection of H_2O_2. The well A1 represented the wild type and other wells corresponded to the mutants. The deeper purple indicated possible positive mutant.

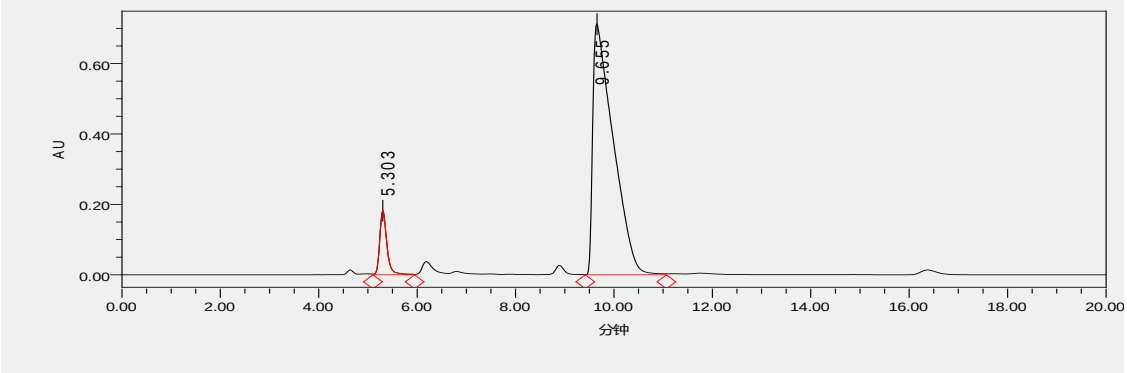

(a)

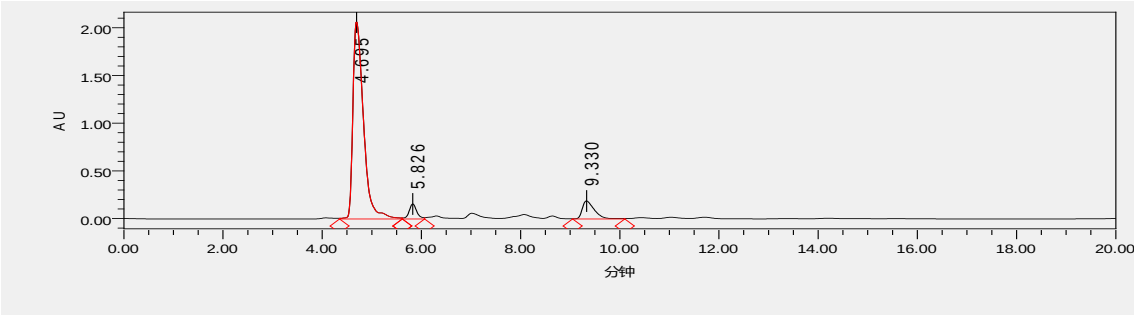

(b)

Figure S6. HPLC chromatogram of methyl glycolate (a) and methyl glyoxylate (b). The retention times for methyl glycolate and methyl glyoxylate were 9.665 and 4.695 min, respectively.